Video Article

Ultrathin Porated Elastic Hydrogels As a Biomimetic Basement Membrane for Dual Cell Culture

Amanda S. Pellowe[1], Holly M. Lauridsen[1], Rita Matta[1], Anjelica L. Gonzalez[1]

[1]Biomedical Engineering, Yale University

Correspondence to: Anjelica L. Gonzalez at anjelica.gonzalez@yale.edu

URL: https://www.jove.com/video/56384
DOI: doi:10.3791/56384

Keywords: Bioengineering, Issue 130, Biomaterials, Basement Membrane, Polyethylene-glycol, Micro-pore, Bilayer, Elastic Hydrogels

Date Published: 12/26/2017

Citation: Pellowe, A.S., Lauridsen, H.M., Matta, R., Gonzalez, A.L. Ultrathin Porated Elastic Hydrogels As a Biomimetic Basement Membrane for Dual Cell Culture. *J. Vis. Exp.* (130), e56384, doi:10.3791/56384 (2017).

Abstract

The basement membrane is a critical component of cellular bilayers that can vary in stiffness, composition, architecture, and porosity. *In vitro* studies of endothelial-epithelial bilayers have traditionally relied on permeable support models that enable bilayer culture, but permeable supports are limited in their ability to replicate the diversity of human basement membranes. In contrast, hydrogel models that require chemical synthesis are highly tunable and allow for modifications of both the material stiffness and the biochemical composition via incorporation of biomimetic peptides or proteins. However, traditional hydrogel models are limited in functionality because they lack pores for cell-cell contacts and functional *in vitro* migration studies. Additionally, due to the thickness of traditional hydrogels, incorporation of pores that span the entire thickness of hydrogels has been challenging. In the present study, we use poly-(ethylene-glycol) (PEG) hydrogels and a novel zinc oxide templating method to address the previous shortcomings of biomimetic hydrogels. As a result, we present an ultrathin, basement membrane-like hydrogel that permits the culture of confluent cellular bilayers on a customizable scaffold with variable pore architectures, mechanical properties, and biochemical composition.

Video Link

The video component of this article can be found at https://www.jove.com/video/56384/

Introduction

Extracellular matrices (ECM) make up the protein scaffolds that support cell attachment and serve as barriers between distinct cell types and are an essential component of complex tissues and organs. In contrast to interstitial connective tissue, the basement membrane (BM) is a specialized type of ECM that acts as a barrier to divide tissue compartments from one another. BMs are approximately 100 µm thick, and therefore allow for direct and indirect communication between cells on either side. Two common examples of BMs are vascular BMs, found in the microvascular wall between pericytes and endothelial cells, and airway BMs that are found between endothelial and epithelial cells. BMs serve an important role in regulating cell function, such as cell polarity and migration, in health and disease.[1] The composition, stiffness, architecture, and porosity of BMs varies across organ systems to facilitate distinct physiological functions. For example, BM pores are critical for maintaining cell-cell communication, soluble molecule diffusion, and for migration of immune cells during inflammation or bacteria during infection. In the airways, pores span the full thickness of the BM, with diameters ranging from 0.75 to 3.86 µm.[2]

The thin nature of the BM ensures that although cell types are physically separated from one another, intercellular communication via paracrine- and contact-mediated signaling is preserved. Thus, to study human disease *in vitro,* researchers have relied on porous permeable support inserts to culture cellular bilayers.[3] These models have been critical for understanding the cellular communication that plays a role in health and disease.[3,4,5,6,7] Permeable support inserts satisfy the basic requirements for understanding how cell-cell signaling regulates physiological processes, such as leukocyte recruitment and bacterial infiltration; however, the inserts have significant limitations and fail to mimic a human BM. Permeable support inserts lack both mechanical and biochemical tunability, and the simplistic porous structure does not mimic the fibrous structure that creates the irregular pores typical of BMs. Therefore, there is a growing need for tunable systems that can recreate the native BM properties that influence cellular processes.

Polymer-based substrates are ideal candidates for the development of biomimetic BMs to study cellular bilayers in a context that more closely mimics the *in vivo* environment.[8,9,10,11,12] Polymers are mechanically tunable and can be chemically modified to incorporate biomimetic peptide fragments.[11,12,13] The bioinert polymer polyethylene glycol (PEG) can be used to construct biomimetic BMs, and recent work has detailed the synthesis of mechanically tunable PEG arginine-glycine-aspartic acid (RGD) gels with porous networks that support cell growth and inflammatory cell chemotaxis.[14] Although published PEG-based substrates provided a more realistic model of a human ECM than permeable supports, many of these models are extremely thick, with a depth of roughly 775 µm that limits the ability to create bilayer cultures with cell-cell contacts.[14]

Here, we present a protocol for the creation of a PEG polymer-based BM mimic that overcomes many of the limitations of current cell bilayer culture technologies. We have developed a templating method that incorporates zinc oxide, an extensively used material for the manufacture of microcrystalline production, into the polymer during synthesis and crosslinking, which is subsequently and selectively removed from the resulting

bulk polymer. This process generates a random porous network, mimicking the tortuous and interconnected pore network of human BMs. Further, the porosity can be altered by changing the size and shape of the zinc oxide microcrystals via modification of the reaction stoichiometry during needle production. The technique developed here creates an ultrathin hydrogel that mimics the thickness of human BM. Lastly, the mechanics, the porosity, and the biochemical composition of these BM-like constructs can easily be altered to generate a microenvironment that is most similar to that seen *in vivo*.

Protocol

Please read Material Safety Data Sheet (MSDS) of all materials prior to use and use safety precautions at all times.

1. Synthesis of Zinc Oxide Needles

1. Prepare 250 mL of a 0.04 M $Zn(NO_3)_2*6H_2O$ solution by adding 2.9749 g of zinc nitrate to 250 mL of water.
2. Prepare 150 mL of 1 M NaOH by adding 6 g of NaOH to 150 mL of water.
3. Set up a mineral oil bath on a hot plate with stirrer, and submerge a 500-mL round bottom flask into the oil bath at room temperature.
4. Add 250 mL of $Zn(NO_3)_2*6H_2O$ to the flask and begin stirring the reaction.
5. Add 150 mL NaOH solution (a white precipitate will form briefly and then disappear as the two solutions continue to mix). Stir for 2 h uncovered.
6. Heat the flask to 55 - 60 °C and continue stirring for 24 h.
7. Turn off the heat and allow solution to cool to room temperature while stirring.
8. Filter the solution on a Büchner funnel with an 11 µm pore size and allow to dry overnight, uncovered. When the filter paper is no longer wet from the poured solution and a white powder has formed over the funnel holes, the particles are fully dried.
9. Collect ZnO needles and prepare for scanning electron microscopy (SEM) to confirm the needle-like morphology. Briefly, mount carbon tape onto a pin stub and use a metal spatula to smear the ZnO needles onto the carbon tape. Sputter coat with 8 mm iridium at a density of 22.4 g/cm^3 and acquire images at 10 kV.

2. Addition of Sacrificial Zinc Layer on Microscope Slides for HCl Induced Release of PEG

1. Prepare zinc acetate solution by dissolving 1.756 g of zinc acetate in 200 mL of methanol.
2. Clean 3" x 1" plain microscope slides with 70% ethanol and a disposable wipe. Allow to air dry for 10 min.
3. Place a 150-mm glass Petri dish onto a hot plate and preheat to 150 - 160 °C.
4. Using a glass pipet with a pipet bulb, hold the glass slides with tweezers and coat slides by applying 5 drops of zinc acetate, forming a thin layer dispersed on the slide. Allow excess solution to drip back into stock solution.
5. Place the slide in the pre-heated Petri dish (150 - 160 °C) with the zinc acetate coated side facing up. Leave on the hotplate for 15 min.
6. Remove the slide with tweezers and allow it to cool to room temperature. The slide will appear to be coated with white streaks.
7. Remove any excess zinc that is remaining on the slides using a disposable wipe to remove prominent white streaks. The surface should be uniform.
8. Expose the the prepared slides to UV light in a biosafety hood for at least 1 h to ensure sterility.
   Caution: UV light is harmful to eyes and exposed skin. Avoid direct exposure to eyes or skin and turn off electrical supply when not using.

3. Preparation of Silicone Isolators

1. Cut silicone sheet into squares less than 1" x 1" (isolators must be able to fit in a 6-well dish).
2. Punch 8 - 12 mm holes in the center of the squares with a biopsy punch.
3. Autoclave silicone isolators for 20 min at 121.0 °C and 1.12 kg/cm.

4. Preparation of PEG solution and PEG Gel Synthesis

Note: Functionalization and polymerization of PEG has been extensively explored and detailed previously by our lab and others.[8,10,11,13,14,15,16,17]

1. Combine the RGD cell adhesive peptide with acryloyl-PEG-NHS in 50 mM sodium bicarbonate (pH 8.5) at a 1:1 molar ratio to enable functionalization of the amine terminus of the peptide with the acrylate moiety, a biochemical reaction that has been previously characterized to yield greater than 85% efficiency.[17]
2. Prepare photo-initiator by mixing 2,2-Dimethoxy-2-phenylacetophenone with 1-Vinyl-2-pyrrolidone at a concentration of 300 mg/mL.
3. In separate 1.5 mL tubes, weigh out the following: 20 mg of ZnO needles, 12.5 mg of PEG-DA, and 2.5 mg of PEG-RGD.
4. Suspend 20 mg of ZnO needles in 270 µL of 10% FBS/PBS solution; vortex to mix (approximately 15 s).
5. Briefly (<1 s) spin the solution in a benchtop mini centrifuge to bring any ZnO aggregates to the base of the tube.
6. Collect 250 µL from the top of the ZnO solution, to ensure that aggregates remain at the bottom of the tube. Combine with PEG-DA and PEG-RGD to create a PEG solution with approximately 2.5 mM RGD. Vortex to mix (approximately 15 s).
7. Add 2 µL of acetophenone/n-vinyl pyrrolidone photo-initiator and vortex briefly to mix (approximately 5 s).
8. Add 20 µL of the polymer solution along the center of the ZnO coated slides.
9. Slowly lower a second slide on top, with the ZnO coating face down (the PEG solution should be between two ZnO coated layers). Try to prevent the formation of any air bubbles. Move the slides laterally along the major axis to allow any bubbles to escape and to spread the solution to a thin layer. Cover the majority of the slide with the polymer solution. Create a slight overhang with the top slide to ensure that the slides can be pulled apart in later steps.
10. Crosslink the slides under a 365 nm UV lamp (approximately 10 mW/cm^2) for 15 min.

5. Release of PEG Gels from Glass Slides

1. Apply pressure to the overhanging slide and manually pull the two slides apart at a slow pace in order avoid cracking the slides. Allow the gels to dry for at least 5 min, or overnight.
2. Place the slide in a sterile 25 mm glass Petri dish and gently pour the 1 M HCl solution onto the slide, using only enough to cover the slide (approximately 10 - 20 mL). Gently rock the Petri dish; the gel should begin to lift off the slide as the HCl dissolves the sacrificial zinc coating and needles. Once the gel is free from the slide, pour the HCl back into the stock solution.
3. Rinse the gel by gently pouring approximately 25 mL of 1x PBS into the Petri dish until the slide and gel are submerged. Carefully pour off PBS into a waste container.
4. Gently pour approximately 25 mL of 1x PBS into the Petri dish until the gel is floating in the solution.
5. Using tweezers, carefully slide the silicone isolator under the gel and lift the gel onto it.
6. Transfer the isolator and the gel into a 6-well dish filled with sterile 1x PBS.
7. Repeat this process until all of the gels have been removed from the slides and are soaking in PBS. Expose the prepared gels to UV light in a biosafety hood for at least 1 h to ensure sterility.

6. Seeding Cell Bilayers

1. Prepare A549 cells for seeding. Briefly, rinse a 75 cm^2 flask with 5 mL of 1x PBS, add 3 mL of 0.25% Trypsin-EDTA and let sit for 2 - 3 min at 37 °C.
    1. Mechanically agitate the flask, quench the reaction with 3 mL Dulbecco's Modified Eagle Medium with 10% fetal bovine serum and 1% penicillin-streptomycin, and collect into a 15-mL conical flask. Rinse with an additional 4 mL of complete Dulbecco's Modified Eagle Media and collect into the same conical. Spin cells at 475 x g for 6 min.
2. While cells are spinning down, add a small drop of complete Dulbecco's Modified Eagle Medium to each well of a 6-well plate. Use tweezers to transfer the silicone isolators with the gels into the new 6-well plate, such that the gel is resting on the drop of media. Now that gels are spread into a thin layer, check to ensure that there are no large holes visible to the eye. This should be done immediately prior to cell seeding to avoid drying and cracking of the gels.
3. Resuspend cells in Dulbecco's Modified Eagle Medium with 10% fetal bovine serum and 1% penicillin-streptomycin at a concentration of 6 x 10^5 cells/mL. Add the cell suspension drop wise to the center of the gel, trying to maintain a meniscus in the punched out area of the silicone membrane. Allow cells to adhere for 4 h.
4. After 4 h, add 0.5 mL of Dulbecco's Modified Eagle Complete Medium to the well and incubate overnight at 37 °C to allow for complete adhesion.
5. The following day, prepare HUVECs for cell seeding.
    1. Rinse a 75 cm^2 flask with 5 mL of 1X PBS, add 3 mL of 0.25% Trypsin-EDTA and let sit for 2 - 3 min at 37 °C.
    2. Mechanically agitate the flask, quench the reaction with 3 mL M199 media with 20% fetal bovine serum, 1% penicillin-streptomycin, and 1% growth supplement, and collect into a 15-mL conical.
    3. Rinse with 4 mL of M199 complete media and collect into the same conical. Spin cells at 475 x g for 6 min.
6. While cells are spinning down, add a small drop of complete medium 199 to each well in a new 6-well plate. Place a new silicone isolator in the well with the drop of media in the center of the silicone.
7. Using tweezers, carefully flip the silicone isolator supporting the PEG gel with A549 cells onto the isolator in the new 6-well plate.
8. Resuspend HUVECs at a concentration of 6 x 10^5 cells/mL and add the cell suspension to the center of the flipped gel drop wise, trying to maintain a meniscus on the gel within the punched out area of the silicone membrane. Allow cells to adhere for 2 h.
9. After 2 h, gently add 2 mL of M199 complete media to each well.

7. Immunofluorescence

1. Carefully remove media from gels with a manual pipette and add approximately 500 µL of 4% paraformaldehyde (PFA) to the center of the gel where the cells are seeded. Let sit for 30 min at room temperature.
   Caution: PFA is a toxic chemical; wear protection and ensure handling is done in a biological safety cabinet.
2. Carefully remove the PFA and add approximately 500 µL of 2% BSA in PBS to each gel. Let sit for 1 h at room temperature.
3. Carefully remove BSA. Prepare primary antibodies at a dilution of 1:100 in 2% BSA in PBS, and add 500 µL to each gel. Let sit for 1 h at room temperature. Rinse gently with 500 µL of 1x PBS.
    1. Repeat the same process with the secondary antibodies. Use following antibodies: 1) anti-human CD144 (VE-Cadherin) clone 16B1; 2) anti-human CD324 (E-Cadherin) clone 6714; 3) anti-human CD31 (PECAM-1) clone C-20; 4) anti-A549; 5) anti-mouse FITC; 6) anti-goat Alexa Fluor 647. To visualize F-actin, add 500 µL of Phalloidin (10 µg/mL in PBS) for 20 min.
4. Carefully remove secondary antibodies or phalloidin and add 500 µL of DAPI (0.1 µg/mL) for 20 min. Carefully remove DAPI solution and gently add 1.5 mL of 1x PBS to each well so that gels are in suspension.
    1. Using tweezers and silicone isolators, transfer one gel to a glass slide. Do this for each gel immediately before imaging, and replace gels into PBS solution after imaging.
    2. Alternatively, mount gels using a DAPI mounting medium. Seal well the samples with nail polish, acquire images within 2 days to prevent drying and cracking of the gel. Refer to Table 1 for troubleshooting.

Representative Results

PEG-RGD hydrogels were formed by sandwiching the polymer solution between two sacrificial zinc oxide layers and creating pore templates with zinc oxide needles. Sacrificial zinc oxide components were then removed with hydrochloric acid, generating ultrathin PEG hydrogels with continuous pores (**Figure 1**). The morphology of zinc oxide needles was confirmed by scanning electron microscopy (SEM), and the average length and width were determined to be 3.92 ± 0.089 µm and 0.43 ± 0.02 µm, respectively (**Figure 2A - 2B**). Following the removal of zinc oxide needles, the hydrogel pores were visualized by SEM and characterized (**Figure 2C - 2E**). The average pore density for hydrogels was 176,863 ± 49,532 pores. SEM was also used to visualize and calculate the pore density of a standard 3 µm pore polycarbonate permeable support insert, and the pore density was found to be significantly lower, with approximately 2.51 ± 0.05 pores per square mm (**Figure 2D**, **Table 2**). The average pore diameter in the zinc oxide templated PEG hydrogel was 0.19 ± 0.01 µm, and was significantly smaller than the 3.47 ± 0.21 µm pores observed in the permeable support insert (**Figure 2E**, **Table 2**). Optical coherence tomography was used to acquire both 2- and 3-dimensional images and to determine the thickness of hydrogels floating in 1x PBS (**Figure 3A - 3B**). The average gel thickness was 18.89 ± 3.47 µm (**Table 2**). Gel mechanics were also evaluated by measuring the elastic modulus as previously described, and the average Young's modulus was found to be 96.78 ± 23.92 kPa (**Table 2**).[14]

Immunofluorescence microscopy demonstrates that both endothelial cells and epithelial cells maintain their phenotypic identities after being cultured on ultrathin PEG-RGD hydrogels. Endothelial cells maintained expression of PECAM-1, and epithelial cells stained positively with an anti-A549 antibody (**Figure 4A - 4B**). Both cell types also maintained the ability to form tight junctions. Endothelial cells expressed VE-cadherin at the cell-cell junctions, and epithelial cells expressed E-cadherin (**Figure 4C - 4D**). The PEG-RGD hydrogels also support cellular bilayers, and allow for cell-cell contacts to form within the porous structures, as demonstrated by immunofluorescent imaging of phalloidin stained samples (**Figure 4E**).

Figure 1. Schematic Overview of Hydrogel Preparation Protocol. A) Synthesis and collection of ZnO needles. **B)** Preparation of glass slides; creation of a sacrificial ZnO layer. **C)** Preparation and sterilization of silicone isolators. **D)** Preparation of PEG solution with ZnO needles. **E)** Polymerization of PEG gels between ZnO coated glass slides. White lines represent sacrificial ZnO needles and coatings. **F)** HCl rinse for the removal of needles and release of gel from slides. Dark lines represent pores created by dissolved ZnO needles. **G)** Transfer of gels and silicone isolators to 6-well dish to prepare for cell seeding. **H)** Cell seeding. Please click here to view a larger version of this figure.

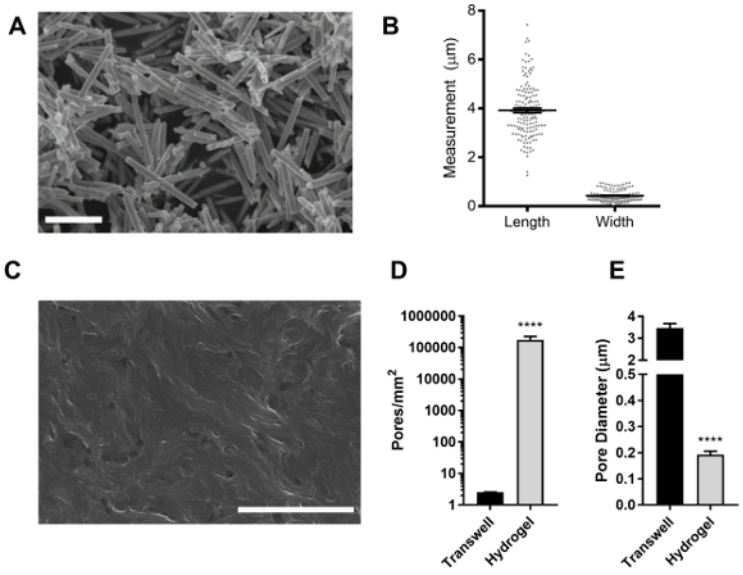

Figure 2. Zinc Needle Characterization and Hydrogel Porosity. A) SEM image of zinc needles (scale bar 5 µm). **B)** Length and width of zinc needles. Dots represent measurements for individual needles; lines represent mean and standard error. **C)** SEM image of porous hydrogel (scale bar 2 microns). **D)** Pore density and **E)** average pore diameter for polycarbonate permeable supports and PEG hydrogels. Bars represent mean and standard error. **** p<0.0001 via T-test. Please click here to view a larger version of this figure.

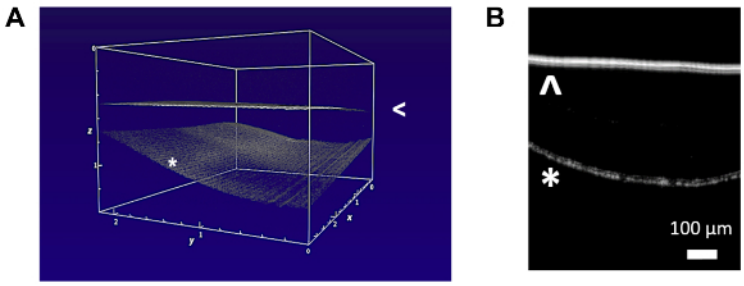

Figure 3. Hydrogel Thickness. Optical Coherence Tomography demonstrates **A)** 3-dimensional and **B)** 2-dimensional images of hydrogels floating in PBS. Arrows represent liquid surface, asterisk represents hydrogel. Scale bar is 100 µm. Please click here to view a larger version of this figure.

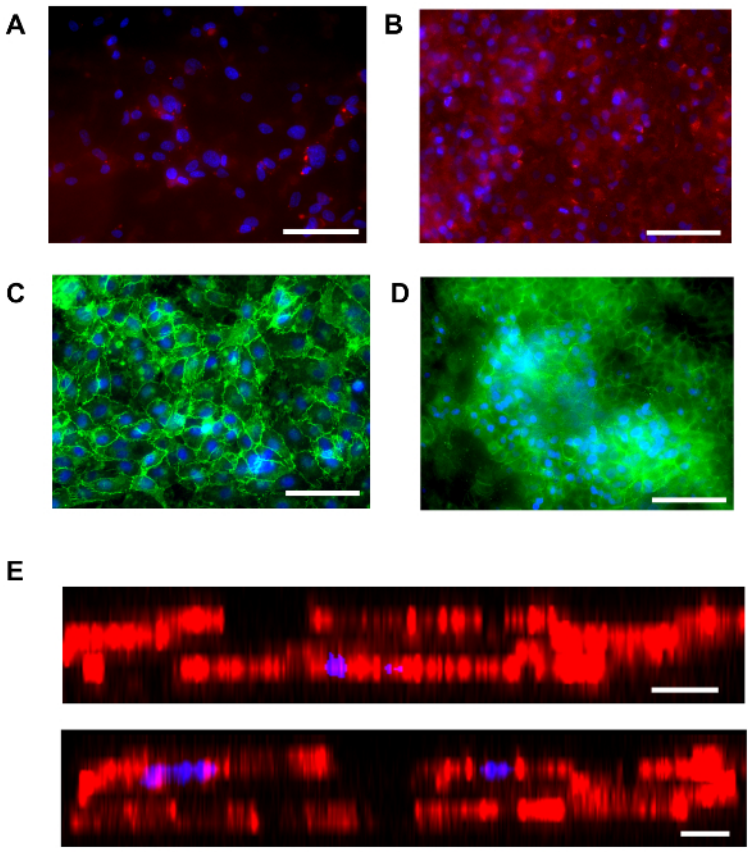

Figure 4. Hydrogels Support Monolayer and Bilayer Culture. Both endothelial cells and epithelial cells are able to form confluent monolayers on PEG hydrogels, as demonstrated by fluorescent staining for **A)** CD31 (CD31 red, DAPI blue) and **B)** A549 (A549 red, DAPI blue), respectively. Formation of intact cadherin junctions are demonstrated for **C)** endothelial cells (VE cadherin green, DAPI blue) and **D)** epithelial cells (E cadherin green, DAPI blue) (scale bars 100 microns). **E)** Two examples of cellular bilayers are demonstrated by phalloidin staining (phalloidin red, DAPI blue) (scale bars 10 μm). Please click here to view a larger version of this figure.

Problem	Potential Solution
Gels have large holes.	Make sure that zinc needles are sufficiently broken up before using them. It might help to use a mortar and pestle to break them up. Make sure that large aggregates are removed with a quick spin following suspension in dilute FBS.
Gel is stuck to the bottom of 6-well plate after seeding cells.	Add a drop of media underneath the gel before transferring into the 6-well plate for seeding.
Gel is covering both the top and the bottom of the silicone isolator.	For longer gels, wrap any excess gel around the silicone isolator to ensure that there is only a single layer in the center where the cells will be seeded.
Cell layer is popping off of gel.	Cells may be over-confluent. Seed at a lower density. Be VERY careful with all rinse steps. You can also increase the peptide concentration to enhance cell adhesion.
Cells are not proliferating very quickly and will not reach confluence.	Seed cells at a high density so that they are near confluence at the time of seeding.
Gel stiffness is higher than expected.	Decrease the amount of time that the gel is kept in HCl.
Gel thickness is higher than expected.	Make sure that any ZnO aggregates are wiped off of the glass slides before casting PEG gel to ensure that slides are smooth. Move slides along the major axis to spread the PEG solution more.

Table 1. Suggested Solutions for Troubleshooting Problems.

	Hydrogel	Transwell	Extracellular Matrix
Pore density (pores/mm^2)	1.77 x 10^5 ± 4.9 x 10^4	2.51 ± 0.05	8.50 x 10^2 to 7.0 x 10^4 [2,14]
Pore diameter (μm)	0.19 ± 0.01	3.47 ± 0.21	0.47 to 3.86 [2,14]
Thickness (μm)	18.89 ± 3.47	10	0.05 to 0.10 [17]
Young's modulus (kPa) [5]	96.78 ± 23.92	>1000	3.5 [14]

Table 2. Comparison of Hydrogel Properties to Standard Permeable Support Insert and Extracellular Matrix (Values Represent Mean ± Standard Error)

Discussion

The protocol detailed here has allowed us to create a tunable PEG hydrogel to serve as a biomimetic BM scaffold. Specifically, by varying PEG molecular weights, peptide conjugation strategies, and zinc oxide microcrystalline structures or concentrations, the elastic modulus, biochemical properties, and porous structure of the hydrogels can be modified, respectively. The ultrathin PEG scaffold features a higher pore density and a smaller pore diameter that is more mimetic of the features found in *in vivo* basement membranes compared to a standard permeable support model (**Table 2**). Further, through this method we have achieved an ultrathin structure with an average thickness of less than 20 μm. While the polycarbonate permeable support models have already achieved an ultrathin layer of just 10 μm, to our knowledge, this is the first free-floating and tunable hydrogel system to achieve this thickness. Lastly, the PEG hydrogels have an elastic modulus of approximately 100 kPa, which is orders of magnitude less stiff than traditional permeable supports, tissue culture plastic, and glass, which all have elastic moduli in the range of GPa, and therefore are more comparable to the low (<10 kPa) elastic modulus of *in vivo* extracellular matrix (**Table 2**).

Achieving a low elastic modulus was one of the primary goals of the work presented here, and is one limitation to the use of traditional polycarbonate permeable support models. It is well known that substrate stiffness can dictate cell behavior, and work has shown that substrate stiffness can guide cellular fate of differentiating cells.[12] Stiff substrates are also commonly used to mimic disease states, including fibrotic tissue or cancerous tumors, and therefore are not accurately representative of healthy tissues.[18,19,20,21] In order to study quiescent cellular phenotypes and functions, it is critical to use substrates that mimic an elastic modulus that is relevant *in vivo*. One of the major advantages of this system is the ability to tune the mechanics of the gel, which can be achieved by using PEG with different molecular weights. As many diseases are associated with ECM stiffening, this system provides a biomimetic platform for studying the effects of healthy versus diseased BM on cell function. Further modification of this system can also be achieved by altering the peptide fragment included for cell adhesion. For the purposes of this study, RGD was used due to its ubiquitous expression in many BM proteins and its ability to facilitate firm cell attachment. In addition to RGD, laminin fragments can also be incorporated to promote laminin-epithelial interactions that guide apical-basal cell polarization.[1] Just as the BM stiffness is altered in disease, the composition of the basement membrane is remodeled in pathological conditions. Using the amine-reactive PEG-NHS precursor, it is possible to conjugate a variety of peptides and proteins to the PEG polymer base.[11,14,15] This is especially advantageous for investigating the effects of integrin engagement for different integrin receptors. For example, the RGD sequence that is expressed in fibronectin and collagen engages multiple integrins, but has a high specificity for integrin αvβ3. To specifically mimic a fibronectin rich substrate, the leucine-aspartic acid-valine (LDV) sequence could be incorporated to engage α4β1, or to mimic a collagenous membrane, aspartic acid-glycine-glutamic acid-alanine (DGEA) could be added to engage integrin α2β1.[8]

Endothelial-epithelial bilayers are just one example of a cellular bilayer that can be created with the model presented here. Other bilayers that exist naturally *in vivo*, separated by only a thin BM or ECM, include endothelial-pericyte and endothelial-smooth muscle cell bilayers. Thus, the applications for this method are broad and extend from pulmonary medicine to vascular biology. Further, because of the unique porosity of these hydrogels, they offer the ability to conduct functional studies that previous hydrogel models have not been able to support. By incorporating pores into our ultrathin hydrogel system, we have created an enhanced biomimetic replacement for permeable support models, enabling the investigation of bacterial infiltration, a common occurrence across the pulmonary epithelial-endothelial barrier in Tuberculosis.[3,6,14,22] Similarly, transmigration or chemotaxis of inflammatory cells across vascular cell cultures can be investigated by measuring the rate of cell capture on the RGD functionalized cell adhesive surface of the gel, as has been shown previously.[16] This is a distinct advantage over previous hydrogel based methods that have achieved co-culture conditions via encapsulation. Such systems allow for close proximity and cell-cell contact between two cell types and have been successful for measuring functions such as angiogenesis and vasculogenesis, but lack the accessibility offered by two-dimensional systems, which provide a much simpler platform for measuring leak, infiltration, or active migration across a co-cultured cellular barrier.[17]

Thus, the method demonstrated here offers a platform for a wide variety of studies across multiple fields, and provides a stepping stone toward generating more relevant data from *in vitro* studies to further understand *in vivo* pathologies and mechanisms.

Disclosures

The authors have nothing to disclose.

Acknowledgements

The authors would like to thank Prof. Paul Van Tassel and Prof. Chinedum Osuji for their thoughtful conversations and materials science expertise. Funding for this work was provided by the Dubinsky New Initiative Award and National Institutes of Health NIBIB BRPR01 EB16629-01A1.

References

1. Domogatskaya, A., Rodin, S., & Tryggvason, K. Functional diversity of laminins. *Annu Rev Cell Dev Biol.* **28**, 523-553 (2012).
2. Howat, W. J., Holmes, J. A., Holgate, S. T., & Lackie, P. M. Basement membrane pores in human bronchial epithelium: a conduit for infiltrating cells? *Am J Pathol.* **158**, 673-680 (2001).
3. Lauridsen, H. M., Pober, J. S., & Gonzalez, A. L. A composite model of the human postcapillary venule for investigation of microvascular leukocyte recruitment. *FASEB J.* **28**, 1166-1180 (2014).
4. Mul, F. P. *et al.* Sequential migration of neutrophils across monolayers of endothelial and epithelial cells. *J Leukoc Biol.* **68**, 529-537 (2000).
5. Hermanns, M. I., Unger, R. E., Kehe, K., Peters, K., & Kirkpatrick, C. J. Lung epithelial cell lines in coculture with human pulmonary microvascular endothelial cells: development of an alveolo-capillary barrier in vitro. *Lab Invest.* **84**, 736-752 (2004).
6. Birkness, K. A. *et al.* An in vitro tissue culture bilayer model to examine early events in Mycobacterium tuberculosis infection. *Infect Immun.* **67**, 653-658 (1999).
7. Wang, L. *et al.* Human alveolar epithelial cells attenuate pulmonary microvascular endothelial cell permeability under septic conditions. *PLoS One.* **8**, e55311 (2013).
8. Pellowe, A. S., & Gonzalez, A. L. Extracellular matrix biomimicry for the creation of investigational and therapeutic devices. *Wiley Interdiscip Rev Nanomed Nanobiotechnol.* **8**, 5-22 (2016).
9. Peyton, S. R., Raub, C. B., Keschrumrus, V. P., & Putnam, A. J. The use of poly(ethylene glycol) hydrogels to investigate the impact of ECM chemistry and mechanics on smooth muscle cells. *Biomaterials.* **27**, 4881-4893 (2006).
10. West, J. L. Protein-patterned hydrogels: Customized cell microenvironments. *Nat Mater.* **10**, 727-729 (2011).
11. DeLong, S. A., Gobin, A. S., & West, J. L. Covalent immobilization of RGDS on hydrogel surfaces to direct cell alignment and migration. *J Control Release.* **109**, 139-148 (2005).
12. Engler, A. J., Sen, S., Sweeney, H. L., & Discher, D. E. Matrix elasticity directs stem cell lineage specification. *Cell.* **126**, 677-689 (2006).
13. Taite, L. J. *et al.* Bioactive hydrogel substrates: probing leukocyte receptor-ligand interactions in parallel plate flow chamber studies. *Ann Biomed Eng.* **34**, 1705-1711 (2006).
14. Lauridsen, H. M., Walker, B. J., & Gonzalez, A. L. Chemically- and mechanically-tunable porated polyethylene glycol gels for leukocyte integrin independent and dependent chemotaxis. *Technology.* **02**, 133-143 (2014).
15. DeLong, S. A., Moon, J. J., & West, J. L. Covalently immobilized gradients of bFGF on hydrogel scaffolds for directed cell migration. *Biomaterials.* **26**, 3227-3234 (2005).
16. Lauridsen, H. M., Gonzalez, A.L. Biomimetic, ultrathin and elastic hydrogels regulate human neutrophil extravasation across endothelial-pericyte bilayers. *PLOS one.* **12**, e0171386- e0171405 (2017).
17. Peters, EB., Christoforou, N., Leong, KW., Truskey, GA., West, JL. Poly(Ethylene Glycol Hydrogel Scaffolds Containing Cell-Adhesive and Protease-Sensitive Peptides Support Microvessel Formation by Endothelial Progenitor Cells. *Cellular and Molecular Bioengineering.* **9**, 38-54 (2016).
18. Schwartz, M. P. *et al.* A synthetic strategy for mimicking the extracellular matrix provides new insight about tumor cell migration. *Integr Biol (Camb).* **2**, 32-40 (2010).
19. Booth, A. J. *et al.* Acellular normal and fibrotic human lung matrices as a culture system for in vitro investigation. *Am J Respir Crit Care Med.* **186**, 866-876 (2012).
20. Kalluri, R. Basement membranes: structure, assembly and role in tumour angiogenesis. *Nat Rev Cancer.* **3**, 422-433 (2003).
21. Roudsari, L.C., Keffs, S.E., Witt, A.S., Gill, B.J., West, J.L. A 3D Poly(ethylene glycol)-based Tumor Angiogenesis Model to Study the Influence of Vascular Cells on Lung Tumor Cell Behavior. *Scientific Reports.* **6**, 1-15 (2016).
22. Bermudez, L. E., Sangari, F. J., Kolonoski, P., Petrofsky, M., & Goodman, J. The efficiency of the translocation of Mycobacterium tuberculosis across a bilayer of epithelial and endothelial cells as a model of the alveolar wall is a consequence of transport within mononuclear phagocytes and invasion of alveolar epithelial cells. *Infect Immun.* **70**, 140-146 (2002).

